East African Rift Dynamics

Moulouda KHAFFOU[1], *Mohamed RAJI*[1], *Moha EL-AYACHI*[2]

[1] Laboratory Applied Geology Geoinformatics, and Environment (GAGE) Hassan II University Faculty of Sciences Ben M'Sick, Casablanca.

[2] Geodesy and Topography Laboratory (GT)/ College of Geomatics Sciences and Surveying Engineering / NELGA NA Program Hassan II Agronomic and Veterinary Institute, Rabat.

Abstract. The East African Rift (EAR) is a typical site for the study of dynamic processes leading to continental break-up and dislocation. In the context of global plate motion models, the kinematics of EAR system is less well defined. In this study, the analysis of repeated GPS geodetic data represents a quantum leap in accuracy that allows us to reassess the recent kinematics of EAR. Our results show that the Somali plate rotates at a velocity of 0.076°/m in the Nubian fixed reference frame the velocity increasing from south to north. We also found that the seismotectonic parameters of both sets of plate boundaries are embodied by lithospheric thinning and oceanic accretion, including a scissor-shaped opening. Normal faults are active along a series of fissure boundaries. This Nubian-Somalian divergence across the East African rift system implies a redistribution of deformation and stress regulation along rift segments connecting rigid blocks that allows for the heterogeneity of the East African basement. We also note the presence of very high-risk seismic zones.

Index Terms— East African Rift (EAR), GPS data, Microplate, Tectonic.

1. Introduction

The East African Rift (EAR) is a lithospheric scale tear. It is located from the Gulf of Aden in the north to the south of Mozambique, dividing the African plate into two unequal parts: the Nubian and Somali plates. EAR system exists for over 30 million years and extends over more than 6,000 km in length and 40 to 60 km in width [1-3]. EAR consists of a series of sequences of tectonic basins aligned several thousand kilometers, separated from each other by relative highs-bottoms, and usually bordered by lifting shoulders. In the north, the estate is mature with advanced oceanic extension. The median transition zone corresponds to the Afar region, where the rupture of the lithosphere begins and the rift valley is completely covered with volcanic rocks. However, to the south, the rate of extension is low, the faults are young and produced in a vast area, and are structured in two sets of rifts.

1.1 Structural framework: The complex geology of the East African Rift, characterized by various structures (Fig.1)

1.1.1 The structural branches

The structural branches are mainly associated with other branches:

● The eastern branch: corresponds to ditch oriented NS to NNE. It consists of four main segments: The Afar Depression, Ethiopian Rift, Kenyan Rift, and Northern Tanzanian divergence.

● Western branch: It consists of the Lake Albert, Lake Edward, Lake George, and Lake Kivu ditches, a central segment, including the Lake Tanganyika and Lake Rukwa ditches.

● Southern segments: including the Lake Malawi ditch and extending south through the Shire River Valley ditch the Dombes and Urema ditches and the South Mozambique ditch located in the oceanic domain. This eastern branch has orthogonal or oblique extension [4].

● South East branch: it extends into the ocean domain, corresponding to the Pangani rift segment, which forms the eastern part of the northern Tanzanian divergence. From north to south, it includes the Pemba, Mafia, Kerimbas, and Lacerda ditches.

● The South Complex: This structure is NE-SW oriented, starting with the Luangwa ditch, the Karroo (Permo-Trias) basin reactivated to the Cenozoic, then the Kariba Lake ditch, and ending in the south west by the half-graben of the Okavango Delta of the Pleistocene.

The south east ditch and the southern complex were born recently from EAR during its spread, as the tectonic corridors of Mweru, Wantipa, and Upemba are future rift opening ditches composed of NE – SW oriented edge faults.

1.1.2 The transverse faults

This corresponds to the assembly of fault segments forming NW-SE orientation zones, partitioning the other rift branches, and themselves composed of small sets of faults. They occupy the regions of Assoua, Tanganyika-Rukwa-Malawi (T.R.M.) [5,6], and Zambezi.

1.1.3 The topographical domes

They are defined by a large amplitude, counted as two: the Ethiopian dome to the north, and the dome of Kenya to the south. These reflect the deep presence of one or two large active mantellic plumes. These data indicate the presence of two mantle plumes, the East African and Afar plumes, which dynamically support the East African and Ethiopian plateaus. Rifting across plateaus is accompanied by the generation of large volumes of basaltic magma [7].

1.1.4 Lakes

The region is also characterized by more than 40 lakes, with very variable dimensions and morphology generally elongated from a few kilometers to several hundred kilometers in length.

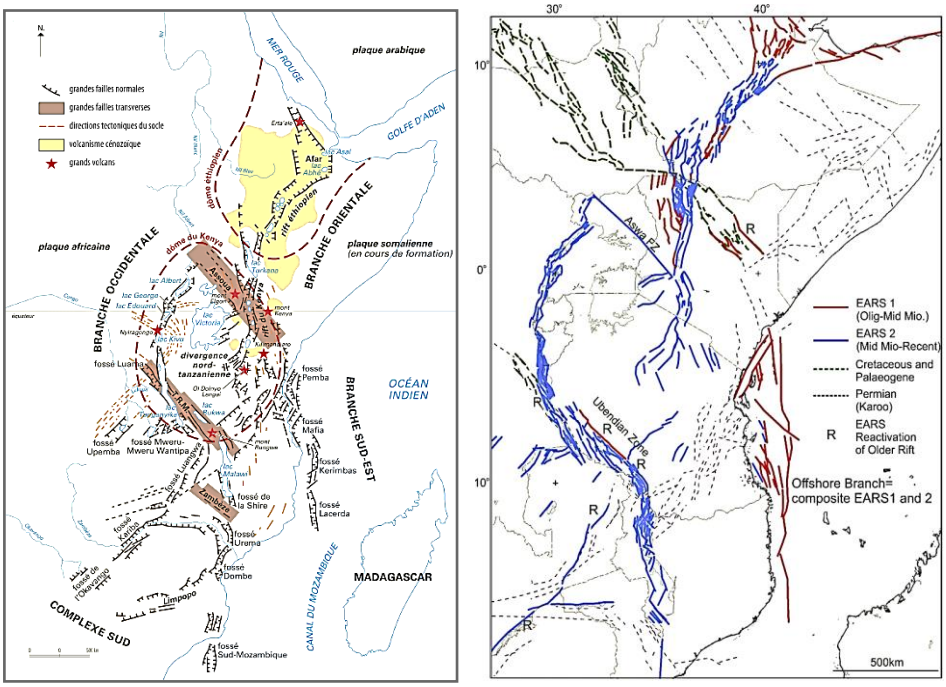

Fig. 1. The structural diagram of the East African Rift showing the major tectonic basins and domes of Ethiopia and Kenya with periods of rift splitting

1.2 Geodynamic context

The geodynamic analysis and synthesis of EAR system determine its deformation, which is associated with hydrothermal volcanic activity on the one hand, and the existence of internal mantellic plumes spotted by the formation of domes on the other surfaces. This active extensive system is divided into two rifting cycles during the Cenozoic. The first is Cretaceous-paleogenic, eo-oligocene to the middle Miocene, which correspond to the creation of 1st EAR which reaches its peak. And the second is Middle Miocene to the upper, corresponding to the creation of the 2nd EAR in the western branch. Thus, there seems to be a trend towards southern youth. These two rifts are framed by the Victoria microplate, which marks an anti-clockwise rotation that generates a time shift of the local extension along the overlapping rift branches.

This edge-driven rotation is due to the shearing of the main plates along the northwest and southeast corners of the microplate where a strong crack has failed, and the cratonic lithosphere transmits this motion and diverts the propagation of the rift branches surrounding the Victoria microplate. The formation of new faults and cracks along the old faults indicates that the separation of Nubian and Somalian plates can cause earthquakes [8].

The East African fault system can be considered a succession of graben basins bound by intracontinental [9], which depends on three factors: the plume of the St Helena mantle ascending, oceanic spreading on the western and eastern margins of the African plate, and heterogeneity within the African continent [10, 11]. However, the birth of EAR was accompanied by the observation of folds, subsidence, and sedimentation in most of the basins of the Plio-Pleistocene age.

Several geodetic and geophysical studies are carried out to follow the kinematics of active tectonics, and provide an accurate mapping of EAR movements. Although these

studies agree, from a point of view, that over a period of several tens of millions of years, an intra-continental dorsal system, including an axial rift, and the spreading of the seabed will progress along the entire length of the rift valley. The ocean will flow, and as a result the African continent will divide into two micro-continents.

2. Methodology

To achieve our research objective, we used the analysis of graphs of the temporal position record (NASA JPL products) and the processing of all angular velocities and uncertainties from approximately 26 permanent GPS sites and the latitude and longitude records of the GPS site positions. These allowed us to describe recent geological movements, to track the kinematics of active tectonics, and thus to provide accurate mapping of recent movements of EAR relative to a rotation-free reference frame (MORVEL model) (Fig. 2).

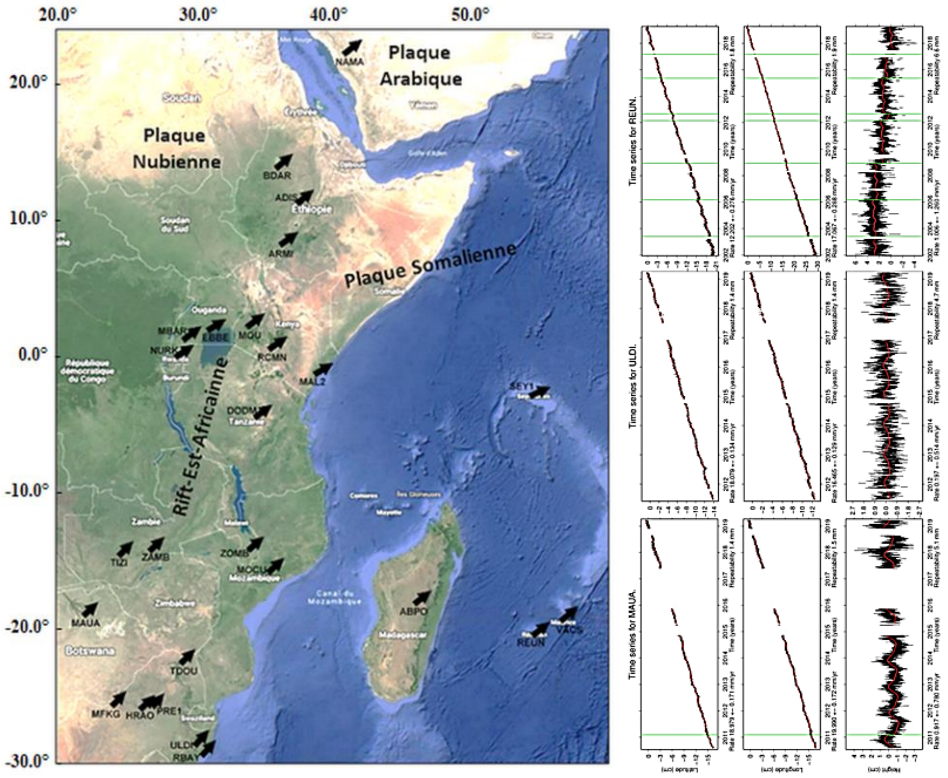

Fig. 2: Right: Representation of GPS velocities in a fixed reference frame in Nubia along the East African Rift (The study area). Left: An example of a permanent GPS site recording latitude, longitude, and position.

3. Resultas

3.1. Geodetic and geophysical solution

Global positioning system (GPS) techniques using spatial geodesy have become widespread since the early 1990s. A fine analysis of the data of the permanent sites makes it possible to show that the speeds agree nearly 99% with the theoretical model of the tectonics of the plates, which represents an average over the last three million years. EAR System is an active extension structure. The divergent plate boundary between Nubia and Somalia is often cited as a modern archetype for rifting and continental rupture; its current kinematics is the least known of any major plate boundary. Analysis of previous studies shows that the average and azimuthal spreading rates of the transform faults along the south-west Indian Ridge improve the kinematic model, which includes three sub-plates (Victoria, Rovuma, and Lwandle) between Nubia and Somalia from 3.2 Transformation Myr [12]. The slip rate of the two plates, Nubia and Somalia, is slow (~5 mm/year), and shows a coherent movement with internal deformations of less than ~1-2 mm/year [13]. Seismicity is present throughout EAR, locally marked by earthquakes of high magnitude (between 6 and 6.5). Large earthquakes occur in the western rift which extends from northern Tanzania to Lake Malawi [5, 6]. While micro seismic activity characterizes the eastern rift. This process was accompanied by superficial manifestations along the rift valley in the form of volcanism and seismic activity with a relatively small magnitude. The important hydrothermal activity in many regions also testifies to the continuity of rift activity. Geophysical data support the concept that a diaper of relatively low-density material is located below the rift system. A combination of seismic refraction and gravimetric data suggests a low-density body of 3.15 g/cm^3 (versus 3.35 g/cm^3 for the cold lithosphere) under the Kenyan rift, and the P wave velocity of 7.5 km/s from 20 to 60 km deep. It has a lateral extent of 200 to 250 km. This is consistent with seismic results indicating that the crust under the rift is thinned at 20 km (from a normal of 36 km for the surrounding East Africa) and at an abnormally low sub-Moho speed [14]. Interpretation of geodetic, gravimetric, and seismological data shows that the average rate of crack growth south of EAR is 2.5 to 5 cm per year, rift opening speeds vary from 2-3 millimeters to 3-4 centimeters per year, the internal deformation of East African System is 0.5 mm/year and the residue is also marked as low on the Nubia plate (mm/year), which is less than 0.5 mm/year.

3.2. Use of Position Record Graphs Over Time and Transform Azimuths and Spreading Rate Data

In our study, we selected 26 permanent GPS stations. From the slope of the NS and EW components of the position time series, it is possible to calculate the mean horizontal speeds of GPS sites over the time period considered. They usually show separately the NS, EW and UP components of the site position for a more intuitive interpretation. To extract the actual (or absolute) speed of each station resulting from the two speeds, the Pythagorean Theorem is used: BC2 = AB2 + AC2 (Table 1).

Site	N	E	V	SN	SE	SV
APBO	14.559	18.817	-0.707	0.172	0.185	0.743
ADIS	18.755	24.509	-1.375	0.183	0.202	0.798
ARMI	19.004	26.555	-3.083	0.284	0.348	1.305
BDAR	17.440	22.300	-0.238	0.582	0.704	2.677
DODM	17.504	23.746	-0.740	0.295	0.341	1.271
EBBE	15.536	25.190	-6.256	0.624	0.753	2.759
HRAO	18.546	17.496	0.795	0.080	0.078	0.327
MAL2	16.104	26.259	-0.033	0.133	0.154	0.566
MAUA	18.974	19.986	0.913	0.170	0.171	0.775

MBAR	17.567	24.279	0.051	0.134	0.155	0.556
MFKG	19.591	18.207	1.176	0.226	0.227	0.911
MOCU	17.132	19.202	-0.821	0.654	0.724	2.714
MOIU	18.393	24.319	-1.033	0.155	0.175	0.685
NAMA	27.347	34.499	0.077	0.169	0.174	0.706
NURK	17.743	25.296	-2.887	0.251	0.297	1.061
PRE1	18.578	17.647	-0.275	0.290	0.290	1.127
RBAY	17.775	16.218	0.144	0.127	0.127	0.544
RCMN	17.361	26.731	-2.187	0.262	0.308	1.147
REUN	12.192	17.063	0.991	0.275	0.288	1.259
SEY1	10.869	25.453	-1.548	0.196	0.204	1.010
TDOU	17.906	17.936	0.448	0.260	0.276	1.108
TEZI	19.161	19.587	1.748	0.399	0.472	1.686
ULDI	19.161	16.461	0.189	0.134	0.128	0.512
VACS	11.235	17.182	-0.929	0.082	0.085	0.370
ZAMB	18.520	20.003	0.578	0.096	0.112	0.419
ZOMBI	17.197	20.129	-0.031	0.299	0.337	1.470

Table 1: Latitude and longitude in degrees with errors in mm. Height estimates and errors in mm. Velocity estimates and errors in mm/yr (2020).

From these calculated results, which are combined with the spatial data, the scrolling speeds, the directions with uncertainties of a sigma, and ellipses of 2 D speed error are calculated; a sigma propagated from MORVEL covariances and the unit of millimeters per year (Table 2). The earthquake, slip vectors, and transform fault azimuths were modeled as the direction of relative motion between the two plates on either side of the block boundary to which the data belongs. Similarly, the oceanic spreading rates were modeled as the velocity of the relative motion between the two plates on either side of the block boundary. The appropriate entries for the plot velocity vector crosses "psvelo" GMT to be plotted using the "- Se" option. The north speed uncertainties were 1-D. IT converts these 3D uncertainties into 2D uncertainty by "psvelo" control and displays speed uncertainty ellipses (Table 3). We estimate that the sites move linearly with time. Thus, the slope of the NS and EW time series directly provides the two horizontal components of the current speed of the Somali plate. In our model (Tables 2 and 3), the representation of these speeds allowed the current movements of the main tectonic plates to be directly visualized.

Site	ong. (E)	Lat. (N)	Taux (mm/an)	Azimut (CW de N)	Semi-majeur axe (mm/an	Demi-mineur axe (mm/a)	Axe majeur orientation CCW de l'est
APBO	47.200	-19.020	2,9 ± 0,6	123,2 ± 5,9	0.9	0.4	137.5
ADIS	38.760	9.040	5,9 ± 0,6	95,7 ± 4,4	0.9	0.5	142.6
ARMI	37.560	6.060	5,6 ± 0,6	94,6 ± 4,7	0.9	0.5	141.3
BDAR	37.360	11.600	6,2 ± 0,6	93,9 ± 4,3	0.9	0.5	143.7
DODM	35.740	-6.180	4,1 ± 0,5	93,2 ± 6,6	0.9	0.5	136.6
EBBE	32.440	0.038	4,9 ± 0,5	88,0 ± 5,9	0.9	0.5	138.0
HRAO	27.680	-25.890	1,6 ± 0,3	62,2 ± 21,6	0.9	0.4	128.7
MAL2	40.190	-2.100	4,7 ± 0,6	99,4 ± 5,3	0.9	0.5	138.8
MAUA	23.530	-19.900	2,6 ± 0,3	61,6 ± 13,2	0.9	0.5	127.7
MBAR	30.740	-0.600	4,8 ± 0,5	85,6 ± 6,1	0.9	0.5	137.3
MFKG	25.540	-25.810	1,7 ± 0,3	55,1 ± 19,9	0.9	0.4	127.6
MOCU	36.840	-16.870	2,7 ± 0,5	97,7 ± 9,4	0.9	0.4	134.4
MOIU	35.290	0.290	4,9 ± 0,5	92,0 ± 5,6	0.9	0.5	138.7
NAMA	42.040	19.210	6,9 ± 0,6	98,2 ± 3,7	0.9	0.6	146.9

NURK	30.090	-1.940	4,7 ± 0,5	84,5 ± 6,4	0.9	0.5	136.5
PRE1	28.220	-25.750	1,6 ± 0,3	64,5 ± 21,6	0.9	0.4	129.1
RBAY	32.080	-28.800	1,0 ± 0,4	77,6 ± 32,1	0.9	0.4	130.6
RCMN	36.890	-1.220	4,7 ± 0,5	94,4 ± 5,6	0.9	0.5	138.5
REUN	55.570	-21.210	3,4 ± 0,6	138,8 ± 5,1	0.9	0.4	139.7
SEY1	55.480	-4.670	5,0 ± 0,6	120,3 ± 3,5	0.9	0.4	140.3
TDOU	30.380	-23.080	1,8 ± 0,4	77,0 ± 17,3	0.9	0.4	130.6
TEZI	26.020	-15.750	3,0 ± 0,4	71,8 ± 11,0	0.9	0.5	130.1
ULDI	31.420	-28.290	1,1 ± 0,4	74,3 ± 30,0	0.9	0.4	130.4
VACS	57.500	-20.290	3,6 ± 0,6	139,2 ± 4,8	0.9	0.4	140.1
ZAMB	28.310	-15.430	2,9 ± 0,4	77,0 ± 10,8	0.9	0.5	131.2
ZOMBI	35.330	-15.380	2,9 ± 0,5	93,6 ± 9,3	0.9	0.4	134.1

Table 2:Illustrates travel speeds relative to the Nubian plate, rates, azimuths and expected uncertainties

Site	Vitesse_east	Vitesse_north	Sig_e	Signe	Corr_ne
APBO	2.4	-1.6	0.5	0.5	-0.6417
ADIS	5.9	-0.6	0.5	0.5	-0.4623
ARMI	5.6	-0.4	0.5	0.5	-0.4740
BDAR	6.2	-0.4	0.6	0.5	-0.4301
DODM	4.1	-0.2	0.5	0.5	-0.5449
EBBE	4.9	0.2	0.5	0.5	-0.4744
HRAO	1.4	0.7	0.4	0.5	-0.5988
MAL2	4.6	-0.8	0.5	0.5	-0.5517
MAUA	2.3	1.2	0.4	0.5	-0.5413
MBAR	4,8	0.4	0.5	0.5	-0.4644
MFKG	1.4	1.0	0.4	0.5	-0.5867
MOCU	2.7	-0.4	0.5	0.5	-0.6085
MOIU	4.9	-0.2	0.5	0.5	-0.4969
NAMA	6.8	-1.0	0.6	0.5	-0.4145
NURK	4.6	0.4	0.5	0.5	-0.4689
PRE1	1.4	0.7	0.4	0.5	-0.6011
RBAY	1.0	0.2	0.4	0.5	-0.6246
RCMN	4.7	-0.4	0.5	0.5	-0.5207
REUN	2.2	-2.5	0.5	0.5	-0.6296
SEY1	4.3	-2.5	0.5	0.5	-0.6394
TDOU	1.8	0.4	0.5	0.5	-0.6017
TEZI	2.8	0.9	0.5	0.5	-0.5339
ULDI	1.0	0.3	0.4	0.5	-0.6216
VACS	2.4	-2.8	0.5	0.5	-0.6266
ZAMB	2.9	0.7	0.5	0.5	-0.5492
ZOMBI	2.9	-0.2	0.5	0.5	-0.5942

Table 3: Plate speed output for psvelo GMT

4. Discussion and conclusion

EAR is considered a typical environment of active continental extension of rafting neoformation, consisting of at least three microplates (Lwandle, Rovuma, and Victoria). Tensile deformation occurs along the deformation zone of each microplate [12, 15, 16] Our geodynamic study used a new dataset combining episodic GPS measurements, with a particular focus on the study of the movement of the Somali plate in relation to the Nubian

plate and along EAR (Fig. 3). The spatio-temporal evolution of this divergent plate boundary is beginning to unravel thanks to a recent increase in geodetic data space in Africa [17, 18, 19]. We found that the sliding vectors provided information that significantly reduced the uncertainties in the plate angular velocity, which estimated and informed us about the role of magmatic processes in extension. The calculated angular velocity for the Somali plate relative to the Nubian plate was estimated to be 35.31° north and 146.16° east. The movement of the two plates is thus described by a rotation pole located at the SE of Africa, with an hourly rotation of 0.076°/ Ma. This rotation explains the divergence along in scissors format, with speeds increasing from south to north. The continuity of the divergence of the Somali plate from the Nubian plate increased over time, which resulted in intense seismic activity from north to south. Tectonic structures indicate that the early stages of rafting will appear with earthquakes triggered by continental crust deformation. This study is consistent with other recently published experiments that show that the evolution of the amount of opening along inferred from geodetic data is associated with an evolution of sub- underlying seismic activity that reflects the evolution of the extension style.

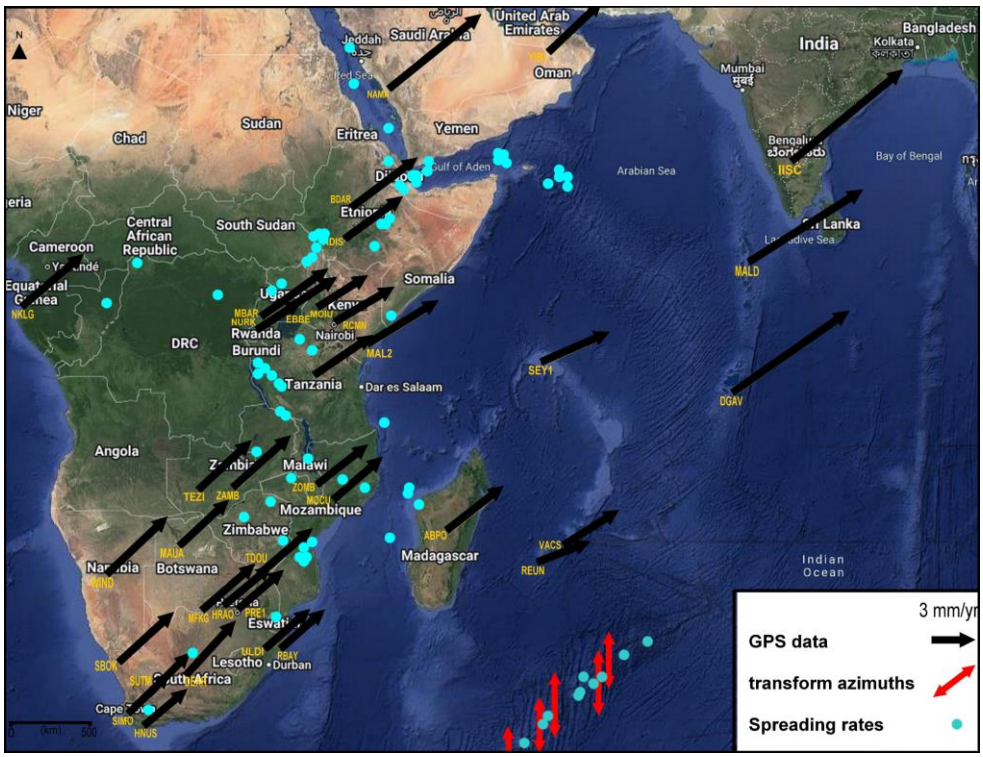

Fig. 3. Kinematic model for the East African Rift System, representing the predicted plate motions in a reference frame set by Nubia. The orientation of the vectors indicates the deformation of the area in a scissor format. The small blue circles are seismicity data from the International Seismological Centre (2021) [18, 19].

Acknowledgment

This work was carried out in collaboration with the Laboratory of Geodynamics of Old Chains LGCA and the Geodesy Laboratory of the Hassan II Agronomic and Veterinary Institute. We thank all my dear teachers for the comments and constructive feedback which

have improved this manuscript. We also thank the services of NASA's Jet Propulsion Laboratory California Institute of Technology for providing geodesic datasets and material used in this study.

References

1. Hirsch, B., et al., (2009), Le Rift- est-africain, une singularité plurielle, IRD Éditions, Chapitre 1 : Géophysique du Rift, Institut de recherche pour le développement, publications scientifiques du MNHN Marseille, p 23- 40.
2. Fournier, M., et al, (2010), Naissance d'un océan, la dorsale de Sheba, GEOPHYSIQUE, Pour la Science - n° 390, p 44-49.
3. Min, G., and Hou,G., (2018), Geodynamics of the East African Rift System 30 Ma ago: A stress field model, Journal of Geodynamics, p 1-11.
4. Corti, G., et al, (2007), Tectonic inheritance and continental rift architecture: Numerical and analogue models of the East African Rift system, TECTONICS, VOL. 26, TC6006, doi:10.1029/2006TC002086, p 3-12.
5. Lavayssière, A., et al, (2019), Depth Extent and Kinematics of Faulting in the Southern Tanganyika Rift Africa, American Geophysical Union AGU, Volume 38, p 1-34.
6. Heilman, E, et al, (2019), Controls of Basement Fabric on the Linkage of Rift Segments, American Geophysical Union, p 4-54.
7. Rogers, N.W., (2015), Basaltic magmatism and the geodynamics of the East African Rift System, Department of Earth Sciences, CEPSAR, The Open University, Walton Hall, Milton Keynes, MK7 6AA, UK, p 79-90.
8. Glerum, A., (2020), Victoria continental microplate dynamics controlled by the lithospheric strength distribution of the East African Rift, NATURE COMMUNICATIONS. https://doi.org/10.1038/s41467-020-16176-x
9. Chorowicz, J., (2005), The East African rift system, Laboratoire de Tectonique, Universite´ Paris 6, Journal of African Earth Sciences 43, p 379–410
10. Min, G., and Hou, G., (2019), Mechanism of the Mesozoic African rift system: Paleostress field modeling, Journal of Geodynamics, p 1-12.
11. Muirhead, J.D., (2019), Rift evolution in regions of low magma input in East Africa, Earth and Planetary Science Letters 506 p 332–346.
12. Stamps, D. S., et al, (2008), A kinematic model for the East African Rift, , Geophys. Res. Lett., 35, L05304, doi:10.1029/2007GL032781, P 1-6.
13. Stamps, D.S., Saria, E. & Kreemer, C. A Geodetic Strain Rate Model for the East African Rift System. Sci Rep 8, 732 (2018). https://doi.org/10.1038/s41598-017-19097-w
14. Saemundsson, K., (2010), East African Rift System - An overview, United Nations University, ISOR – Iceland GeoSurvey Grensásvegur 9, 108 Reykjavík ICELAND, p1-6.
15. Fernandes, R.M.S., Delvaux, D., Miranda, J.M., Saria, E., and Stamps, D.S., 2013, Re-evaluation of the kinematics of Victoria block using continuous GNSS data: Geophysical Journal International, v. 193, p. 1–10, https://doi.org/10.1093/gji/ggs071.
16. Saria, E., Calais, E., Delvaux, D., Hartnady, C.J.H., and Stamps, D.S., 2014, Present-day kinematics of the East African Rift: Journal of Geophysical Research: Solid Earth, v. 119, p. 3584–3600. https://doi.org/10.1002/2013JB010901.
17. Deprez A. ,et Al., (2013), Seismic and aseismic deformation along the East African Rift System from a reanalysis of the GPS velocity field of Africa, Geophysical Journal International, Volume 193, p 1-16.

18. Raphaël Mukandila Ngalula. Analyse des données GNSS de l'Afrique de 1994 à 2017.6: caractérisation de mouvement et déformation active. Sciences de la Terre. Université de Strasbourg, 2020. Français. ⟨NNT : 2020STRAH026⟩. ⟨tel-03813763⟩
19. D.S. Stamps, C. Kreemer, R. Fernandes, T.A. Rajaonarison, G. Rambolamanana. Redefining East African Rift System Kinematics. Geology, 49 (2), (2020), pp, 150-155,